J Mater Sci (2008) 43:4236–4246
DOI 10.1007/s10853-008-2613-2

Analytical study of tensile behaviors of UHMWPE/nano-epoxy bundle composites

S. Jana · B. R. Hinderliter · W. H. Zhong

Received: 26 July 2007 / Accepted: 25 March 2008 / Published online: 9 April 2008

Abstract Ultra-high molecular polyethylene (UHMWPE) fiber reinforced nano-epoxy and pure epoxy composites in bundle form were prepared and tested for tensile properties. UHMWPE fiber composites are well known for their superior tensile performance, and this work was conducted to assess the effect of adding nanoadditives to the resin and to evaluate possible enhancements or degradations to that attribute. The results showed that tensile tests on various types of UHMWPE fibers/nano-epoxy bundle composites resulted in an increase in modulus of elasticity due to the addition of small amounts of reactive nanofibers (r-GNFs) to epoxy matrix. It was observed that the modulus of elasticity of the composite bundles depended on both volume fractions of the matrix and the weight percent (wt%) of r-GNFs in the matrix. A non-linear relationship was established among them and an optimal modulus was determined by calculation. A three-dimensional surface plot considering these two parameters has been generated which gives an indication of change in modulus of elasticity with respect to volume fraction of matrix and wt% of r-GNFs in the matrix. A Weibull analysis of tensile strengths for the various bundle composites was performed and their Weibull moduli were compared. The results showed that presence of r-GNFs in the composites increased the strength effectively, and 0.3 wt% r-GNFs based composites showed the highest strength. An important ancillary finding is that optimum tensile values are a function not only of the above parameters, but also strongly influenced by the addition of diluents which control the viscosity of the blend.

S. Jana · W. H. Zhong (✉)
School of Mechanical and Materials Engineering,
Washington State University, Pullman, WA 99164, USA
e-mail: Katie_zhong@wsu.edu

B. R. Hinderliter
Department of Coatings and Polymers, North Dakota State University, Fargo, ND 58105, USA

Introduction

Mechanical properties of a fiber reinforced composite depend on the properties of the fiber and matrix constituents, as well as the interface between the fiber and matrix. The interface is often called the "third constituent" because of its strong influence on the overall composite mechanical properties. Due to exceptional mechanical and physical properties [1] of ultra-high molecular weight polyethylene (UHMWPE) fibers, especially its high efficiency as shielding material [1] against galactic cosmic rays, they are known to be suitable for application in space missions. However, owing to the inertness of the UHMWPE fiber surface, the interfacial adhesion between the fiber and the polymers is inherently poor, and therefore, UHMWPE fiber reinforced polymer composites do not show good overall mechanical properties [2, 3]. To improve their mechanical properties, many surface treatments for UHMWPE fibers, such as nitrogen plasma [4], laser ablation [3], nitrogen ion implantation [4, 5] and chain disentanglement [6, 7], have been investigated; however, these methods could also possibly lower some of the mechanical properties of UHMWPE fibers. Although some other surface treatments such as plasma polymerization [8] and polymer coating (sizing) [9] do not lessen the mechanical properties of UHMWPE fibers, significant extra cost is incurred from these treatment procedures. Instead of performing any modification of the surface of the UHMWPE fibers, we developed a reactive nano-epoxy material as the matrix for the UHMWPE fiber composites

through fabrication a reactive graphitic nanofiber (r-GNF) [10]. In our previous studies, it was shown that the wetting and adhesion properties of the nano-epoxy with the reactive graphitic nanofibers (r-GNFs) to the UHMWPE fibers were improved [11, 12].

Graphitic nanofibers (GNFs) can be produced from ethylene and carbon monoxide in large volume at low cost, which is important for mass production of reinforced composites [13–16]. GNFs have a large number of edges from exposed graphene planes which may be used for addition of functional groups through chemical modification of the surface of GNFs. These functional groups work as bi-functional linkers and assist in generation of covalent bond formation between nanofibers and polymer resin molecules [17, 18]. Much research has been carried out to improve mechanical properties of composites by adding nanoscale fillers, including GNFs, to epoxy resin and/or other polymer matrices [19–28]. However, very few of these efforts reported any improvements to the mechanical properties of UHMWPE/polymer matrix composites using small amount of nanofillers (less than 1 wt%).

In our previous research, functionalized herringbone GNFs with 3,4′-oxydianiline (GNF-ODA) (Fig. 1a) were fabricated into r-GNFs (Fig. 1b) [29–31], in which reactive hydrogen in the group –OH– was involved in the curing reaction with epoxy resins, similar to the function of an amine type curing agent, which then incorporates the nanofibers into the cured matrix structures. The result is an r-GNFs/epoxy unified resin system, i.e. a true matrix, rather than a simple physical mixture, typical of many "nanocomposites" [30, 31]. The r-GNFs were incorporated into the blend with a reactive diluent, butyl glycidyl ether

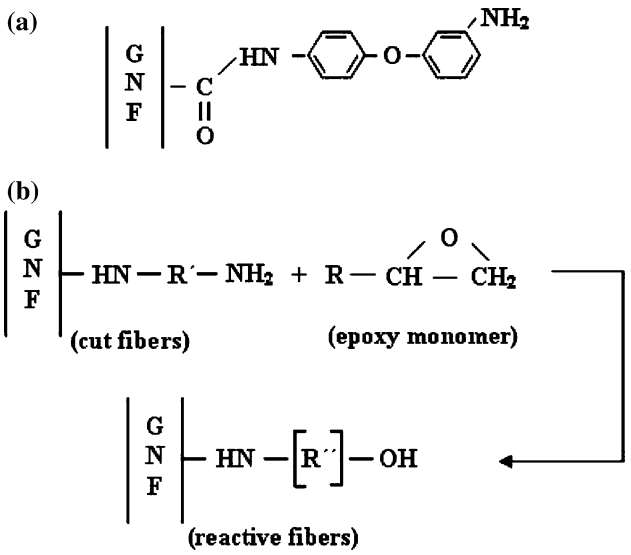

Fig. 1 (**a**) Structure of a GNF-ODA nanofiber (**b**) formation of r-GNF

(BGE). Initially this is used for cutting purposes and has an epoxide group similar to an epoxy resin. Existence of BGE can prevent the highly polarized r-GNFs from agglomeration. However, when used as a diluent, high amounts of BGE can lower the mechanical properties of epoxy resin. Therefore, an appropriate ratio of r-GNFs to the diluent should be applied into the nano-epoxy to achieve optimum mechanical properties for the resulting composites.

Pure epoxy and three groups of nano-epoxy matrices in various ratios (1:4, 1:6 and 1:7) of the r-GNFs to the BGE and each group with various r-GNF contents (0.2, 0.3 and 0.5 wt%) were prepared. UHMWPE fibers were impregnated with these matrices to make UHMWPE fiber/nano-epoxy bundle composites. In this paper we have reported the mechanical properties of the UHMWPE fibers/nano-epoxy composites in a bundle form. To investigate the effect of r-GNF content on mechanical properties of the UHMWPE fiber/nano-epoxy composites, tensile tests were conducted on all types of bundle composites and an analytical study was performed on the tensile behaviors of the composites. We studied the relationship among Young's modulus, volume fraction of matrix, and wt% of r-GNFs. Two-parameter Weibull analysis of the composite tensile strengths was applied and Weibull moduli of different types of composites were compared.

Experimental

The epoxy resin (Epon® 828), curing agent (Epikure™ W Curing Agent), and accelerator (Epikure™ 537 Curing Agent) were provided by Miller Stephenson Chemical Inc. The UHMWPE fiber (Spectra® fiber 1000) was purchased from Honeywell Co. The diluent was butyl glycidyl ether (BGE) purchased from Sigma–Aldrich. Vanderbilt University provided the functionalized graphitic nanofibers, GNF-ODA.

GNF-ODA nanofibers and diluent butyl glycidyl ether (BGE) were mixed in 1:50 ratio by weight and sonicated at room temperature for 3 h with a power level of 70 W. An ice water tank was used for the cooling process. Sonication assisted in shortening the length of GNF-ODA to 400–600 nm; however, there was no change in diameter of GNF-ODA (25 nm) which can be observed from Fig. 2. These GNF-ODA nanofibers were allowed to react with BGE for 36 h to change the GNF-ODA nanofibers to r-GNFs shown in Fig. 1b. The sonicated solutions were placed in a hot vacuum chamber (70 °C) to attain various r-GNFs/BGE solutions with determined ratios of 1:4, 1:6, and 1:7, respectively, by weight.

Epon Resin 828 (DGEBA) was added to the curing agent (Epikure™ W) in 100:24 proportions by weight to get pure-epoxy matrix. r-GNF/BGE solutions were added

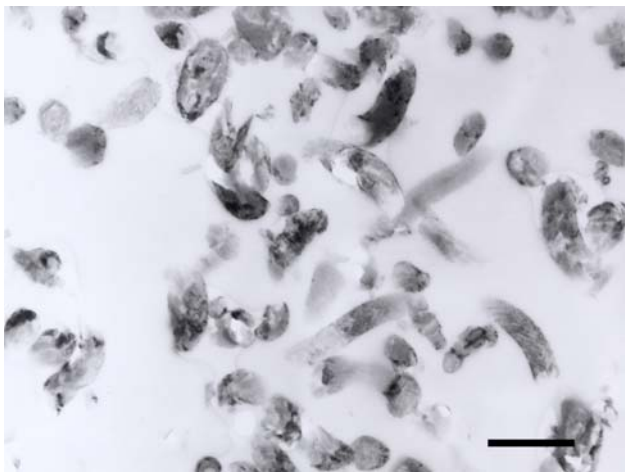

Fig. 2 TEM image of typical nano-epoxy matrix containing well dispersed r-GNF (scale bar: 50 nm)

to pure epoxy matrix to achieve different types of nano-epoxy matrices (0.2, 0.3, and 0.5 wt% r-GNFs by weight) for each group. An accelerator (Epikure^{TM} 537) was added to each matrix in the ratio 1:200 to lower the curing temperature (to avoid melting UHMWPE fiber). For uniform dispersion of r-GNFs into the matrices, a low level sonication was performed for 1 h for each type of matrix at room temperature. All types of pure-epoxy and other three nano-epoxy groups prepared for the UHMWPE fiber bundle composites are listed in Table 1.

Both pure-epoxy and nano-epoxy bundle composites were fabricated by impregnating UHMWPE fibers with each type of matrix solution, cured for 4 h at 120 °C, and then cooled naturally to room temperature. We used an internally developed process and setup to impregnate the UHMWPE fibers into the matrix. UHMWPE fibers were passed through a resin matrix bath and then through a fixed roller system. The pressure between the rollers was held constant for each type of specimen. UHMWPE fiber bundle impregnation was controlled by providing a continuous supply of matrix in the bath before passing through the rollers. The shape of the bundle composites was cylindrical; the diameter of the specimens was 0.37–0.45 mm and areas of cross-section of the specimens were calculated from the diameter. For all kinds of specimens prepared in this study, only a single kind of UHMWPE fiber bundle (120 fibers) was used. The variation in diameter of the specimens is a consequence of the matrix quantities. The matrices consisted of various amounts of epoxy resin, diluent, and r-GNF, and viscosity varied accordingly. Unavoidably, even specimens from the same matrix combination showed differences in diameter. Therefore, utmost caution was taken to segregate the samples into different sections according to groups and diameters. There may have been some voids; however, they were not considered in this study as it is difficult to measure the amount of void in each sample and, moreover, we made the specimens under identical processing system and conditions. The bundle composites were cut into pieces having 12 cm length in which 4 cm (2 cm from each side) of the total length was used for gripping the bundle composite with PMMA plates and epoxy super glue in the tensile tests. All the tensile tests were carried out on a *Q*-test machine of MTS System Corporation with a load cell which has a maximum loading capability of 4,581 N. The loading rate was 1.0 mm/min. The morphology of the tested specimens was observed by scanning electron microscopy (SEM).

Results and discussion

Interpretation of modulus

More than 10 specimens were tested for each type, with load versus displacement curves obtained from the tensile

Table 1 UHMWPE fiber/epoxy and UHMWPE fiber/nano-epoxy specimens prepared for tensile tests

Specimens' group	Bundle specimen code (type)	Description of the matrix used		
		Components of the matrix	wt% of r-GNFs	wt% of diluent
Group pure-epoxy UHMWPE fiber/epoxy	E1-0	Pure epoxy matrix	0	0
Group N4 UHMWPE fiber/nano-epoxy	N4-0.2/0.8	Epoxy + r-GNFs + diluent (r-GNFs:diluent = 1:4)	0.2	0.8
	N-4-0.3/1.2		0.3	1.2
	N-4-0.5/2.0		0.5	2.0
Group N6 UHMWPE fiber/nano-epoxy	N-6-0.2/1.2	Epoxy + r-GNFs + diluent (r-GNFs:diluent = 1:6)	0.2	1.2
	N-6-0.3/1.8		0.3	1.8
	N-6-0.5/3.0		0.5	3.0
Group N7 UHMWPE fiber/nano-epoxy	N-7-0.2/1.4	Epoxy + r-GNFs + diluent (r-GNFs:diluent = 1:7)	0.2	1.4
	N-7-0.3/2.1		0.3	2.1
	N-7-0.5/3.5		0.5	3.5

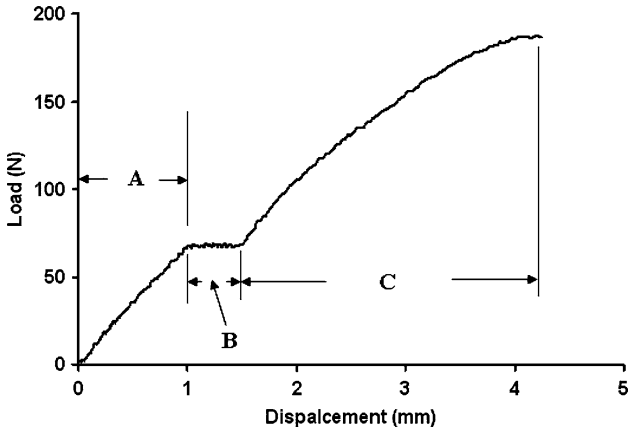

Fig. 3 Typical curve of load versus displacement under tensile loading

tests for analysis. We considered only specimens of the N6 group because they showed the most consistent and improved results among all nano-epoxy bundle composite specimens in their respective concentrations in each aspect (modulus, strength, etc.). It was found that the shapes of the load versus displacement curves of the various composite specimens with different r-GNF loadings and different r-GNF/BGE ratio were similar. Figure 3 is a typical load versus displacement curve of a bundle specimen of UHMWPE fibers reinforced pure epoxy or nano-epoxy composites under tensile loading. This typical curve has three regions: (1) region A which corresponds to the elastic deformation of the bundle composite, (2) region B, a plateau relates to the onset of matrix cracking, micro-crack multiplication, and debonding between the matrices and the UHMWPE fibers, and (3) region C, which reveals the failure of the UHMWPE fibers (a full description and explanation of these regions are available in Ref. [32]). The fractographies of specimens at regions A, B, and C accompanying their image analysis have been provided in [33] in detail.

Modulus of elasticity, a main characteristic of the composite bundle in the elastic region (region A), was calculated using Hook's Law This modulus of elasticity, or Young's modulus, in composites depends upon volume fractions of both matrix and fiber, and is often approximated using the rule of mixture (ROM) (Eq. 1), which neglects possible synergistic effects:

$$E_{\text{comp}} = V_{\text{f}}E_{\text{f}} + (1 - V_{\text{f}})E_{\text{m}} \quad (1)$$

E_{comp}, E_{f} and E_{m} are the moduli of composite, fibers and matrix, respectively. V_{f} is the volume fraction of the UHMWPE fibers. The experimental results for moduli are shown in Table 2. It was found from these results that the modulus of elasticity of the nanocomposites was a function of the nanofiber loadings and volume fractions of resin in the specimens, i.e.

Table 2 Moduli (experimental) of bundle composites with different r-GNF contents

wt% of r-GNF	Volume fraction of matrix	Modulus (GPa)	Standard deviation
0.0	0.67	39.452	5.484
	0.65	36.056	
	0.59	43.193	
	0.58	48.193	
	0.57	47.503	
	0.55	50.059	
	0.54	49.235	
	0.5	50.34	
	0.49	51.147	
	0.46	52.954	
0.2	0.47	56.863	2.891
	0.46	61.112	
	0.45	63.34	
	0.43	62.295	
	0.42	64.452	
	0.4	61.449	
	0.39	66.237	
	0.38	64.593	
	0.37	65.572	
	0.35	66.648	
0.3	0.57	55.502	4.149
	0.55	59.435	
	0.54	60.142	
	0.52	63.398	
	0.51	69.697	
	0.5	65.341	
	0.49	67.037	
	0.48	65.823	
	0.47	64.708	
	0.46	64.961	
0.5	0.44	64.341	1.629
	0.43	64.197	
	0.42	61.755	
	0.41	63.984	
	0.39	60.562	
	0.38	61.917	
	0.37	64.348	
	0.36	62.458	
	0.34	64.624	
	0.33	60.454	

$$E_{\text{comp}} = f(V_{\text{m}},\ \text{wt}_{\text{r-GNF}}) \quad (2)$$

where V_{m} is the volume fraction of matrix and $\text{wt}_{\text{r-GNF}}$ is the wt% of r-GNFs in the matrix, and thus an interrelationship existed between the matrix and the nanoreinforcement. Experimental data of Group N6

(r-GNFs to BGE diluent was 1:6, Table 1) was used to analyze the dependency of the modulus of elasticity on the volume fraction of the matrix and the wt% of r-GNFs in the matrix. From these results of Group N6 specimens, it was assumed that the above function (Eq. 2) would be a non-linear equation as shown below:

$$E_{\text{comp}} = C_1 + C_2 V_{\text{m}} + C_3 \text{wt}_{\text{r-GNF}} + C_4 V_{\text{m}}^2 + C_5 \text{wt}_{\text{r-GNF}}^2 + C_6 V_{\text{m}} \text{wt}_{\text{r-GNF}} + C_7 V_{\text{m}}^3 + C_8 \text{wt}_{\text{r-GNF}}^3 + \cdots \quad (3)$$

where C_i are constants. Procedure "Mnlfit" [34], based on the Levenberg–Marquardt method, was used to fit a function relating modulus of elasticity to two free variables: wt% of r-GNFs, and volume fraction, of matrix to find the above constant values. Modifications were conducted on the Mnlfit procedure according to our requirements. After fitting the data in procedure Mnlfit, we obtained the following equation:

$$E_{\text{comp}} = 30.58 + 58.00 V_{\text{m}} + 135.80 \text{wt}_{\text{r-GNF}} - 104.89 V_{\text{m}}^2 - 188.72 \text{wt}_{\text{r-GNF}}^2 + 28.84 V_{\text{m}} \text{wt}_{\text{r-GNF}} \quad (4)$$

Optimum Young's modulus was calculated from Eq. 4, which depended on both volume fraction of matrix and wt% of r-GNFs in the matrix. Maximum Young's modulus was 66.28 GPa for the volume fraction of matrix: 38.5% and the wt% of r-GNFs: 0.33%. A three-dimensional surface curve was plotted as shown in Fig. 4 considering modulus of elasticity, volume fraction of matrix, and wt% of r-GNFs as coordinates. From this figure, it can be observed that the maximum gradient of curves of modulus versus wt% of r-GNFs in the matrix are lower compared to the maximum gradient of curves for modulus versus volume fraction of the matrix. However, considering all the matrix volume fractions in these experiments, the bundle specimen modulus was highest at 0.3 wt% of r-GNF content (Fig. 4). Therefore the three-dimensional surface curve shows that the addition of r-GNF improved Young's modulus of the UHMWPE fiber/epoxy composite. This improvement can be explained with the effect of proportionate amount of epoxy, BGE, and r-GNF in specimens of 0.3 wt% r-GNF. Epoxy cross-linking network plays a major role in properties' determination in all kinds of specimens, and addition of r-GNF/BGE solution to epoxy resin lessens epoxy concentration, i.e. in cured specimens, density of cross-linking network would be low. On the other hand, r-GNFs form the bondage with epoxy molecules, which in turn mitigate the effect of diminished epoxy cross-linking in specimens to some extent. This scenario can be visualized through a schematic diagram shown in Fig. 5. We know that the addition of r-GNF solution to epoxy matrix affects the epoxy structure two ways: (1) it reduces the epoxy concentration, i.e. cross-linking density

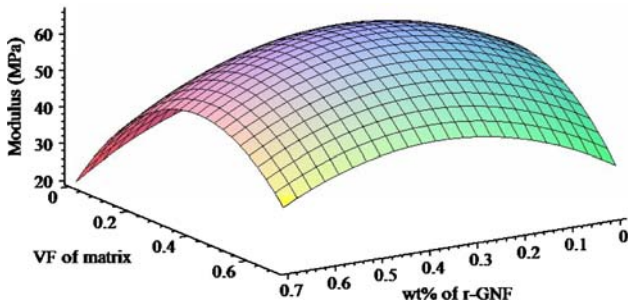

Fig. 4 Three-dimensional surface curve of modulus of elasticity versus volume fraction of matrix versus wt% of r-GNF

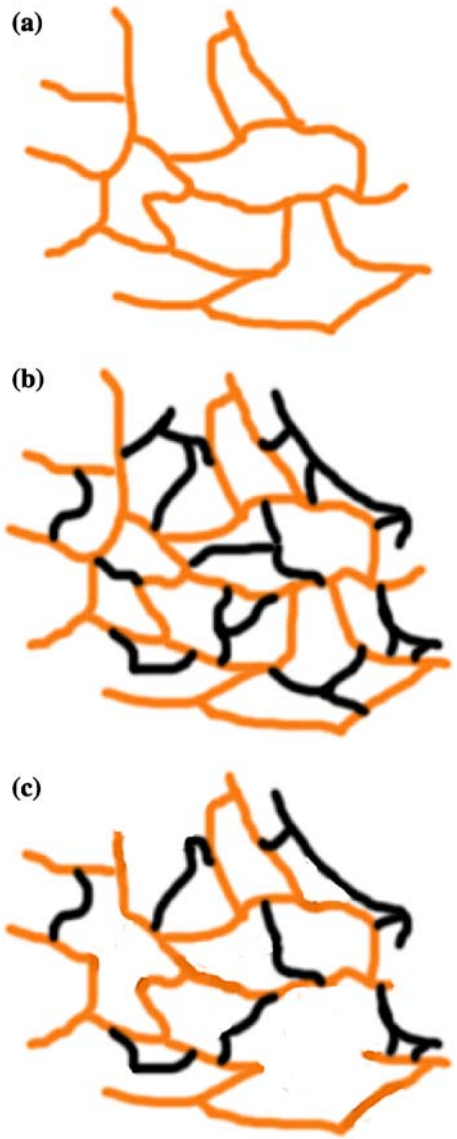

Fig. 5 Schematic diagram of epoxy cross-linking and r-GNF bonds: (**a**) pristine epoxy, (**b**) 0.3 wt% nano-matrix, and (**c**) 0.5 wt% nano-matrix (yellow, epoxy link; black, r-GNF bond)

would be less in the structure and (2) it binds epoxy molecules with themselves at curing which assists in improving the properties. As the mechanical properties of r-GNF are higher than the cured epoxy, it can be expected that addition of r-GNF would improve the properties of epoxy matrix. However, it should be noted that amount of epoxy needs to be proportionate to produce more bonds with epoxy. Considering the results, it is conceivable that in specimens with 0.3% r-GNF, the amounts of epoxy and r-GNF were optimal which formed efficient structure. Whereas in 0.5% r-GNF specimen, the amount of epoxy went down further due to more presence of BGE (as much as twice in 0.5% matrix compared to that in 0.3%). Less amount of epoxy hinders production of r-GNF bonding with epoxy. Therefore, in 0.5%, both the amounts of epoxy cross-linking and r-GNF bindings were less compared to those in specimens with 0.3% r-GNF. The above described possible phenomenon is depicted through a schematic diagram in Fig. 5 in which yellow color stands for epoxy cross-linking and black for r-GNF bonding. In summary, the stoichiometry of the epoxy, BGE, r-GNF should be optimum to manifest improvements in properties in the epoxy system.

Comparison of tensile strength

Tensile strengths of UHMWPE fiber bundle composites with pure-epoxy and nano-epoxy are shown in Fig. 6 as a function of r-GNF contents. In Table 3, standard deviation related to each data point in Fig. 6 has been provided in lieu of error bars to simplify the figure. In the nano-epoxy specimens, experimental data of groups N4, N6, and N7 containing 0.2, 0.3, and 0.5 wt% r-GNFs were taken into consideration in this tensile strength versus r-GNF content graph. Among all the types of specimens, the pure-epoxy composite specimens showed the lowest tensile strength,

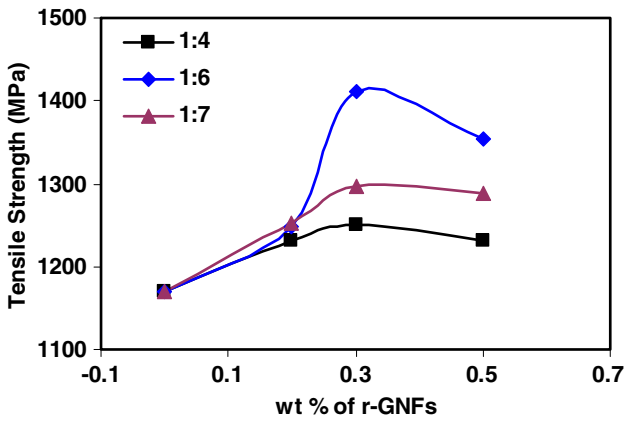

Fig. 6 Tensile strength of bundle composites with different r-GNF content

Table 3 Standard deviation of tensile strength

wt% of r-GNF	N4	N6	N7
0.0	47.64	47.64	47.64
0.2	43.69	42.51	45.29
0.3	37.12	33.23	33.45
0.5	37.23	35.43	34.16

while specimens with 0.3 wt% r-GNFs from the N6 group depicted the highest tensile strength. Also, in each group, specimens with 0.3 wt% of r-GNFs demonstrated the highest strength in its respective group. The increment of tensile strength of specimens of groups N4, N6, and N7 with 0.3 wt% r-GNFs were 7%, 20%, and 11%, respectively, compared to that of pure-epoxy specimens. Consequently, it was speculated that in the plateau stage of the load–displacement curve (Fig. 3), where matrix cracking onset and crack multiplication took place [32, 33], the greater brittleness in pure-epoxy had a major influence on the large numbers of matrix cracks occurring at lower strains and had little influence over the failure of the specimen in stage C. This large number of matrix cracks in a relatively short time in the pure-epoxy, as observed during the tests, resulted in sudden load transfer from the matrix to the fibers, and this caused more fibers to bear the full load from the beginning of the test. On the other hand, the other groups with diluent and r-GNFs which responded with more non-catastrophic behavior led to greater toughness in the material. Moreover the bond between nanofiber and epoxy molecules formed in curing process [30] assisted in blocking the advancement of crack initiation and multiplication as discussed later in detail. This feature might have resulted in fewer cracks in nano-epoxy at the end of plateau stage which in turn helped to increase the tensile strength bearing more load.

In the cure process of nano-epoxy composites, covalent bonds were formed between r-GNFs and epoxy resin [29–31]. At the same time, formation of cross-linking networks in epoxy resin occurred. It could be deduced that in comparison to a matrix without bonding between the nanofillers and the polymer, the nano-epoxy with r-GNFs had greater influence on a larger zone of the epoxy network surrounding the r-GNFs through the existence of the covalent bond between r-GNFs and epoxy resin molecules. This led to larger and stronger interphase zones between the epoxy network and the nanofibers, and at the same time the sum of all the interphase zones offered an improved overall nano-epoxy cross-linking structure, as compared to the pure-epoxy, where cross-linking occurred only among epoxy molecules in the formed epoxy network. As a consequence, mobility of the molecules in the nano-epoxy composites required greater energy compared to that

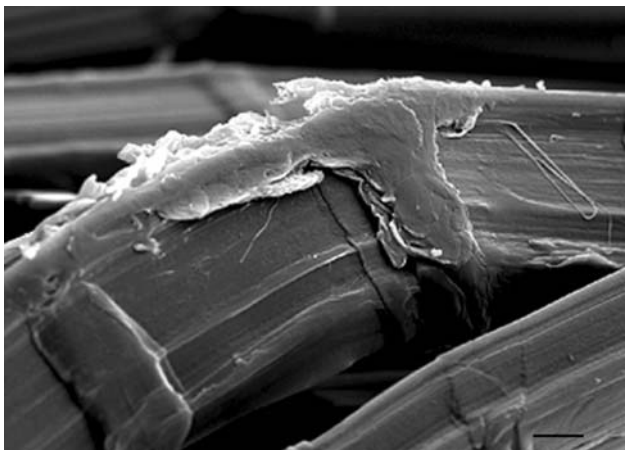

Fig. 7 SEM micrographs showing the failure morphologies of nano-epoxy bundle composite (0.3% of N6 group), scale bar: 10 μm ×1,000

needed in pure-epoxy. This phenomenon can be analyzed from the morphologies from the failed specimens (0.3% concentration of N6 group and pure epoxy). Figure 7 shows that some nano-epoxy matrix attached to the UHMWPE fiber after failure, while in contrast Fig. 8 shows a clean surface of the UHMWPE fiber in the failed composite specimen with pure-epoxy matrix [31]. More analysis and images are in Ref. [33]. In specimens with 0.2 wt% r-GNFs, the amount of diluent and r-GNFs was less compared to specimens with 0.3 wt% r-GNFs, and therefore the nano-matrix with 0.2 wt% r-GNFs had higher viscosity causing less wetting to occur on the UHMWPE fiber surface [11]. Specimens with 0.2 wt% r-GNFs had less r-GNFs compared to specimens with 0.3 wt% and so fewer covalent bonds occurred between r-GNFs and the epoxy molecules compared to specimens with 0.3 wt% of r-GNFs. In specimens with 0.5 wt% r-GNFs, both the amounts of diluent and r-GNFs were high compared to those in specimens with 0.3 wt% r-GNFs and the effect of that higher amount of diluent was to decrease the cross-linking density in the epoxy resin. Specimens with 0.3 wt% r-GNFs of group N6 showed the best result due to the presence of justified amounts of diluent with optimum amounts of nanofibers in this matrix. It also showed good dispersion of r-GNFs in the matrix (Fig. 2), which was a very important factor in improving mechanical properties [35–38].

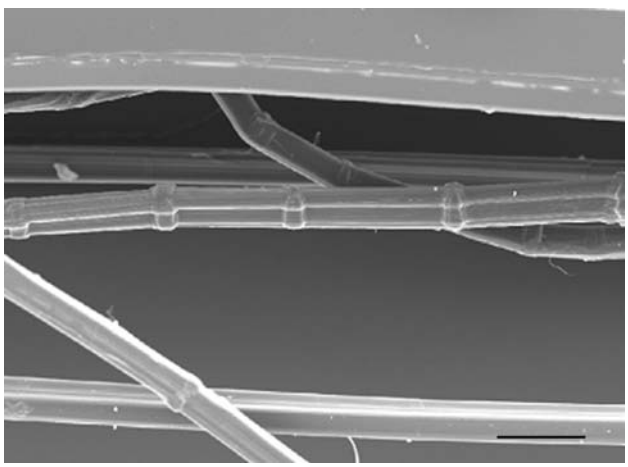

Fig. 8 SEM micrographs showing the failure morphologies of pure-epoxy bundle composite scale bar: 100 μm ×150

Weibull analysis

It was found that each type of composite bundle exhibited a wide variation in tensile strength. Many variables such as the nature of the material, crack sizes, crack spacing, specimen preparation, handling of materials, specimen storage, and experimental technique could affect these strength results [39]. The Weibull distribution is widely used to measure this scatter of strength in brittle and quasi-brittle materials. The failure probability p of different types of bundle composites was studied by a two-parameter Weibull distribution (Eq. 5) [40]. This failure probability generally depends upon volume V of the composite, where V_0 is a reference volume, σ is stress at which failure of composite occurs, β is scale parameter, and m is the Weibull modulus.

$$P = 1 - \exp\left[-\frac{V}{V_0}\left(\frac{\sigma}{\beta}\right)^{m}\right] \tag{5}$$

The lengths of all bundle specimens were equal and their cross-sectional areas were approximately the same. Therefore Eq. 5 can be expressed as Eq. 6

$$P = 1 - \exp\left[-\left(\frac{\sigma}{\beta}\right)^{m}\right] \tag{6}$$

A linear regression method was used to evaluate the Weibull parameters. In each set of tensile strength results of each type of specimen, the lowest to the highest stress values were assigned to a probability of failure based on its ranking, where ranking starts from 1 to n, n is number of specimens in each set. In this analysis we considered 10 specimens for each type and therefore n is 10. The following equation (Eq. 7) was used to evaluate the probability of failure for the rth specimen [41],

$$P = \frac{r - 0.5}{n} \tag{7}$$

By taking logarithms of both sides of Eq. 6, it becomes

$$\ln\left[\ln\left(\frac{1}{1-P}\right)\right] = m\,\ln(\sigma) - m\,\ln(\beta) \tag{8}$$

Equation 8 represents a straight line from which slope (m) and intercept ($m\,\ln(\beta)$) can be measured. Figure 9

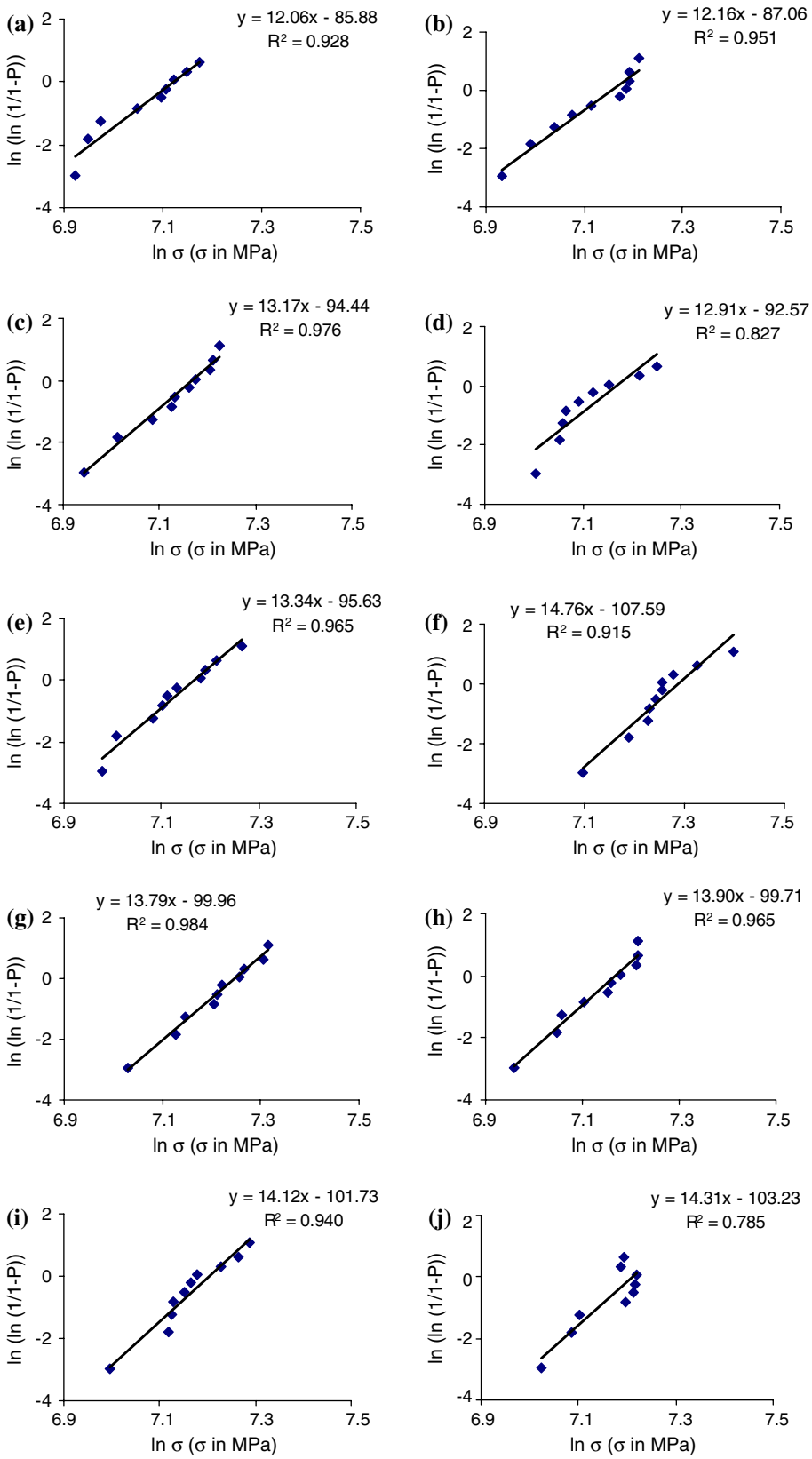

Fig. 9 Weibull plots of bundle composites with different r-GNF contents: (**a**) Pure-epoxy group, (**b**) 0.2 wt% r-GNFs in N4, (**c**) 0.3 wt% r-GNFs in N4, (**d**) 0.5 wt% r-GNFs in N4, (**e**) 0.2 wt% r-GNFs in N6, (**f**) 0.3 wt% r-GNFs in N6, (**g**) 0.5 wt% r-GNFs in N6, (**h**) 0.2 wt% r-GNFs in N7, (**i**) 0.3 wt% r-GNFs in N7 and (**j**) 0.5 wt% r-GNFs in N7

Table 4 Weibull moduli and scale parameter of bundle composites with different r-GNF contents

Specimens' group	Specimen type	m (Weibull modulus)	β (scale parameter) (MPa)
Pure-epoxy	Pure-epoxy	12.06	1,238.48
N4	0.2	12.16	1,281.55
	0.3	13.17	1,299.21
	0.5	12.91	1,298.61
N6	0.2	13.34	1,298.69
	0.3	14.76	1,461.64
	0.5	13.79	1,405.02
N7	0.2	13.90	1,304.43
	0.3	14.12	1,345.02
	0.5	14.31	1,354.67

shows $\ln\left[\ln\left(\frac{1}{1-P}\right)\right]$ versus $\ln(\sigma)$ curves, which indicate that tensile strengths of different types of UHMWPE/nano-epoxy bundle composites follow a Weibull distribution. In Table 4, values of m and β of different bundle composites calculated from linear plots are listed. Generally, m (shape parameter) measures the scatter in strength data or dispersion of the distribution in crack length and is connected to the scatter of relevant crack sizes of fracture and their distances. The higher the value of m, the less scatter of tensile strength of the composite results. In other words, a larger m means a more uniform and narrow flaw distribution. It is seen (Fig. 9) that in some cases, points deviate significantly from the line passing through them. This is likely due to undetected damage done to the composites during specimen preparation. R^2 is the coefficient of determination which is a measure of how well the regression line represents the data. With higher deviations from the nominal line, R^2 is reduced. Usually, the Weibull scale parameter, β, is a measure of the nominal strength of the material and the average strength of the composite will increase with increasing value of β.

The number of specimens is critically important for a Weibull analysis, and as the results of current study follow the Weibull curve quite well, it is believed the results have validity. The lowest value for Weibull modulus m of 12.06 was found for pure-epoxy specimens. The Weibull modulus was consistently higher for bundle composites with high amounts of r-GNFs; the highest value for m is 14.76 for specimens having 0.3 wt% r-GNFs of N6 group. Beyond this point, the value of the Weibull modulus m decreases. This demonstrates that the specimens with 0.3 wt% of r-GNF of N6 were more uniform in strength and had fewer flaws. We already mentioned that these specimens had the presence of justified amounts of diluent with optimum amounts of nanofibers in the matrix and showed the best mechanical properties among all composites. In other non-optimum cases such as the nano-epoxy with 0.2 wt% r-GNF or 0.5 wt% r-GNF, it is thought that either the amounts of r-GNF were too low (in the former case) to have sufficient bonding or had non-optimum amounts of diluent (BGE) with respect to the epoxy network and thus adverse viscosity effects.

We also observed the same phenomenon in the variation of the Weibull scale parameter β with increments of r-GNFs content. The value of β for specimens with 0.3 wt% r-GNF (N6) was 1,461, which is the highest among all composites we tested so far and the lowest was for pure-epoxy composite. The higher m and β values in specimens with 0.3 wt% of r-GNFs of Group N6 specimens indicated that this optimum combination of r-GNFs and diluent not only increased the strength but also reduced the strength scatter compared to pure-epoxy specimens. From this it can be postulated that in addition to r-GNFs increasing the tensile strength of nanocomposites, the appropriate amounts of diluent had the further effect of reducing the scatter. Thus it is concluded that the addition of r-GNF with appropriate amounts of BGE to an epoxy resin improves the tensile properties in UHMWPE fiber reinforced composites by enhancing the matrix properties synergistically.

The values of the Weibull modulus m and Weibull scale parameter β found from tensile test were compared to those found from flexural tests [42]. Identical trends were observed in corresponding parameters in both experiments. However inclusion of bundle fibers in a matrix increased the scattering of strength in bundle composites. Simultaneously, it also enhanced the nominal strength of the composite. The reasons behind these phenomena are explained earlier in this paper and also in Ref. [42].

The other important issue to be discussed is adhesion between the matrix and UHMWPE fibers. For better adhesion, the surface energy of UHMWPE fiber should be higher than that of the matrix. In this experiment, we tried to modify the epoxy resin by adding r-GNF (in diluent BGE which work as reactive agent) to it. The working principle behind this modification has been discussed

earlier in this paper. The surface energy of this polymer matrix decreases compared to original matrix, which has been revealed in our previous studies [11]. Our approach was intended to take the advantage of surface chemistries from the ingredients of nano-epoxy matrix to improve the adhesion between matrix and UHMWPE fiber, and consequently we achieved better adhesion between them with the addition of r-GNF, which also has been reported in our previous studies [10, 12, 31, 31, 43]. Therefore, it is obvious that the improvement of tensile strength comes not only from enhancement of matrix properties but also from increased adhesion between UHMWPE fiber and matrix. However, it is not clear from this study how much of total tensile strength improvement comes from adhesion enhancements. The answer to this query which remains to be revealed might be found out by analyzing the experimental data on molecular scale.

Conclusions

Tensile tests on different types of UHMWPE fiber/nano-epoxy bundle composites were conducted and a Weibull analysis was applied to analyze the effect of r-GNFs on them. It was observed that distinct increases of modulus of elasticity and tensile strength occurred with the addition of r-GNFs in the matrix. A non-linear quadratic equation which shows a relation among modulus of elasticity, volume fraction of matrix, and wt% of r-GNFs was developed. Optimal values of modulus of elasticity with specific volume fraction of matrix and r-GNFs were calculated. A three-dimensional surface curve was generated through the calculations. A two-parameter Weibull analysis was applied to analyze the tensile strength and Weibull moduli of various types of composites and compared. The results showed that the presence of a justified amount of r-GNFs in an appropriate amount of diluent in the composites increased the strength, with 0.3 wt% r-GNFs based composite (N6) showing the highest tensile properties of the UHMWPE fiber composites.

Acknowledgements The authors gratefully acknowledge the support from NASA through the grant NNM04AA62G, Dr. W.H. Zhong also gratefully acknowledges Dr. Charles M. Lukehart and Mr. Jiang Li (Vanderbilt University) for providing the derivatized graphitic carbon nanofibers, and Mr. M. T. Wingert for making contribution to the TEM and SEM imaging work.

References

1. Jang BZ (1994) Advanced polymer composites: principles and applications. ASM International
2. Ujvari T, Toth A, Bertoti I, Nagy PM, Juhasz A (2001) Solid State Ionics 141:225. doi:10.1016/S0167-2738(01)00750-0
3. Torrisi L, Gammino S, Mezzasalma AM, Visco AM, Badziak J, Parys P, Wolowski J, Woryna E, Laska L, Pfeifer M, Rohlena K, Boody FP (2004) Appl Surf Sci 227:1149. doi:10.1016/j.apsusc.2003.11.078
4. Kostov KG, Ueda M, Tan IH, Leite NF, Beleto AF, Gomes GF (2004) Surf Coat Technol 186:287. doi:10.1016/j.surfcoat.2004.03.033
5. Chen JS, Lau SP, Sun Z, Tay BK, Yu GQ, Zhu YF, Zhu DZ, Xu HJ (2001) Surf Coat Technol 138:33. doi:10.1016/S0257-8972(00)01126-9
6. Cohen Y, Rein DM, Vaykhansky L (1997) Compos Sci Technol Vol 57:1149. doi:10.1016/S0266-3538(96)00149-2
7. Wang J, Smith K Jr (1999) Polymer 40:7261. doi:10.1016/S0032-3861(99)00034-8
8. Dilsiz N, Ebert E, Weisweiler W, Akovali G (1995) J Colloid Interf Sci 170:241. doi:10.1006/jcis.1995.1093
9. Drzal L, Madhukar M (1993) J Mater Sci 28:569. doi:10.1007/BF01151234
10. Zhamu A, Wingert MT, Jana S, Zhong WH, Stone JJ (2007) Composites A 38:699. doi:10.1016/j.compositesa.2006.10.001
11. Neema S, Salehi-Khojin A, Zhamu A, Zhong WH, Jana S, Gan YX (2006) J Colloid Interface Sci 299:332 doi:10.1016/j.jcis.2006.02.016
12. Zhamu A, Zhong WH, Stone JJ (2006) Compos Sci Technol 66:2736. doi:10.1016/j.compscitech.2006.03.005
13. Sandler J, Shafter TP, Bauhofer W, Schulte K, Windle AH (1999) Polymer 40:5967. doi:10.1016/S0032-3861(99)00166-4
14. Yue ZR, Jiang W, Wang L, Toghiani LH, Gardner SD, Pittman CU (1999) Carbon 37:1607. doi:10.1016/S0008-6223(99)00041-X
15. Pittman CU, He GR, Wu B, Gardener SD (1997) Carbon 35:313
16. Wong EW, Sheehan PE, Lieber CM (1997) Science 227:1971. doi:10.1126/science.277.5334.1971
17. Chen XH, Wang JX, Yang HS, Wu GT, Zhang XB, Li WZ (2001) Diamond Relat Mater 10:2057. doi:10.1016/S0925-9635(01)00486-1
18. Li J, Vergne MJ, Mowles ED, Zhong WH, Hercules DM, Lukehart CM (2005) Carbon 43:2883. doi:10.1016/j.carbon.2005.06.003
19. Vogelson CT, Koide Y, Alemany LB, Barron AR (2002) Chem Mater 12:795. doi:10.1021/cm990648e
20. Choi YK, Sugimoto K, Song S, Gotoh Y, Ohkoshi Y, Endo M (2005) Carbon 43:2199. doi:10.1016/j.carbon.2005.03.036
21. Zilg C, Dietsche F, Hoffmann B, Dietrich C, Mülhaupt R (2001) Macromol Symp 169(Fillers and Filled Polymers):65
22. Lan T, Cho J, Liang Y, Maul P (2001) Nanocomposites-2001, Chicago, 25–27 June
23. Gilbert EN, Hayes BS, Seferis JC (2002) Nanoparticle modification of epoxy based film adhesives, Proc. SAMPE, Covina, CA, p 41
24. Spindler-Ranta S, Bakis CE (2002) Carbon Nanotube reinforcement of a filament winding resin. Proc. SAMPE, Coniva, CA, p 1775
25. Chen C, Curliss D (2001) SAMPE J 37:11
26. Rice BP, Chen C, Cloos L, Curliss D (2001) SAMPE J 37:7
27. Becker O, Barely R, Simon G (2002) Polymer 43:4365. doi:10.1016/S0032-3861(02)00269-0
28. Becker O, Cheng YB, Varley RJ, Simon GP (2003) Macromolecules 36:1616. doi:10.1021/ma0213448
29. Li J, Vergne MJ, Mowles ED, Zhong WH, Hercules DM, Lukehart CM (2005) Carbon 43:2883. doi:10.1016/j.carbon.2005.06.003
30. Zhong WH, Li J, Xu LR, Lukehart CM (2005) Polym Compos 26:128. doi:10.1002/pc.20085
31. Wingert MT (2004) Improvement of interfacial adhesion between UHMWPE fiber and epoxy matrix using graphitic carbon nano-

fiber, a master thesis, North Dakota State University, Department of Mechanical Engineering
32. Jana S, Zhamu A, Zhong WH, Gan YH (2006) J Adhes 82:1157. doi:10.1080/00218460600998763
33. Jana S, Zhamu A, Gun YX, Zhong WH, Stone JJ (2008) Mater Manuf Process 23:102
34. "http://www.maplesoft.com", Holmgren DE (holmgren@brandonu.ca) Brandon University, Brandon, MB, Canada, Ogilvie JF (ogilvie@munkebo.chem.ou.dk) and Monagan M (monagan@cecm.sfu.ca) Center for Experimental and Constructive Mathematics, Simon Fraser University, Vancouver BC, Canada
35. Johnson JA, Barbato MJ, Hopkins SR, O'Malley MJ (2003) Prog Organ Coat 47:198. doi:10.1016/S0300-9440(03)00139-5
36. Fanelli M, Feke DL, Manas-Zloczower I (2006) Chem Eng Sci 61:473. doi:10.1016/j.ces.2005.07.024
37. Sun CJ, Saffari P, Sadeghipour K, Baran G (2005) Mater Sci Eng: A 405:287. doi:10.1016/j.msea.2005.06.032
38. Qing Z, Frogley MD, Wagner HD (2002) Compos Sci Technol 61:2139
39. Peterlik H (1995) J Mater Sci 30:1972. doi:10.1007/BF00353020
40. Afferrante L, Ciavarella M, Valenza E (2006) Int J Solids Struct 43:5147. doi:10.1016/j.ijsolstr.2005.08.002
41. Quinn G (1990) J Am Ceram Soc 73:2374. doi:10.1111/j.1151-2916.1990.tb07601.x
42. Jana S, Zhong WH, Gan YX (2007) Mater Sci Eng A l445–1446:106
43. Salehi-Khojin A, Stone JJ, Zhong WH (2007) J Compos Mater 41:1163